Calibration procedure of a combined fluorescence-backscattering sensor: the RBR*tridente*

Mathieu Dever
RBR
Ottawa, CANADA
Woods Hole Oceanographic Inst.
Woods Hole, MA, USA
mathieu.dever@rbr-global.com
0000-0002-4292-6368

Jon Taylor
RBR
Ottawa, CANADA
jon.taylor@rbr-global.com

Greg Johnson
RBR
Ottawa, CANADA
greg.johnson@rbr-global.com

***Abstract*—Fluorometers and backscatter sensors are essential tools in oceanography, used to measure various biogeochemical parameters, and are key components of the BGC-Argo program. The RBR*tridente* integrates these two sensors into a single device. In this study, we detail the calibration procedure for the RBR*tridente*, a combined fluorescence-backscattering sensor developed by RBR. The calibration process involves three key steps: gain calibration, temperature compensation, and optical calibration. We describe each step in detail including the methodology for generating primary standards for calibration, as well as the primary and secondary reference instruments used for calibration. The calibration procedure is validated in the field by comparing the measurements of the RBR*tridente* to other fluorometers and backscatter sensors commonly used as part of the BGC-Argo program.**

***Index Terms*—BGC Argo, fluorometer, backscatter, oceanographic sensors, calibration**

I. Introduction

Fluorometers and backscatter sensors are extensively used in oceanography to estimate some of the Essential Ocean Variables (EOVs) established by the international oceanographic community. The key working principle of fluorometers relies on the excitation of a chemical compound at a specific wavelength, followed by the sensing of the amount of light emmitted back at a different, longer, wavelength. By tuning the wavelengths of the excitation/emission pair, fluorometers can be used to measure various biogeochemical parameters, the most common one being chlorophyll-fluorescence to estimate phytoplankton biomass [2], [6]. They are also widely used to measure concentrations of crude oil, cyanobacteria via phycocyanin, red-algae via phycoerythrin fluorescence, and fluorescing Dissolved Organic Matter (fDOM). They can also be used to track dye concentrations, most commonly rhodamine Water Tracer (WT), which helps study water movement and mixing processes.

Because of the similarities in instrument design between fluorometers and backscattering sensors, these two sensors are often combined into a single instrument. Backscattering sensors are used to detect particulate matter in the ocean, another EOV [8], which is a crucial variable to constrain carbon fluxes in the ocean [3]. Unlike fluorometers, the light emitted and measured by the backscattering sensor is limited to the same wavelength. The amount of light reflected back to the sensor's detector is used to estimate the concentration of particles in the measurement volume.

Fluorometers and backscattering sensors are key instruments for the BGC-Argo program, a program set to measure key biogeochemical ocean variables at a global scale [3]. As the BGC-Argo program grows, new sensors and sensor manufacturers are introduced and deployed in the ocean. It is crucial for the continuity of the program and the quality of its data to characterize new sensors, validate their performance in the field, and carefully document the calibration process used by the manufacturers in order to guarantee the inter-comparability of the sensors across manufacturers.

The RBR*tridente*, a combined fluorometer and backscattering sensor, was recently introduced into the BGC-Argo program. In this work, we aim to detail the calibration method used by the manufacturer, RBR, and validate the performance of the instrument in situ, to a depth of 6000 m.

II. Working principle and instrument design

There are many commonalities between fluorometers and backscattering sensors. They are both composed of an emission side, where light is emitted, and a detector side where a light signal is measured with a photodiode. For fluorometers, they are referred to as the excitation and emission sides (Fig. 1). The two cones formed by the illumination from the light source and detector field of view form a three-dimensional measurement volume of 1.3 cm^3 that extends from 0.8 to 26.6 mm from the sensor's face. The characteristics specific to fluorescence and backscattering sensors are detailed below.

A. Fluorescence

The working process begins with a light source, typically an LED, which emits light at a specific excitation wavelength. This light passes through an excitation optical filter, which ensures that only light of the desired wavelength reaches the sample. A reference photodiode is included on the excitation side of the fluorometer to track any drift in the

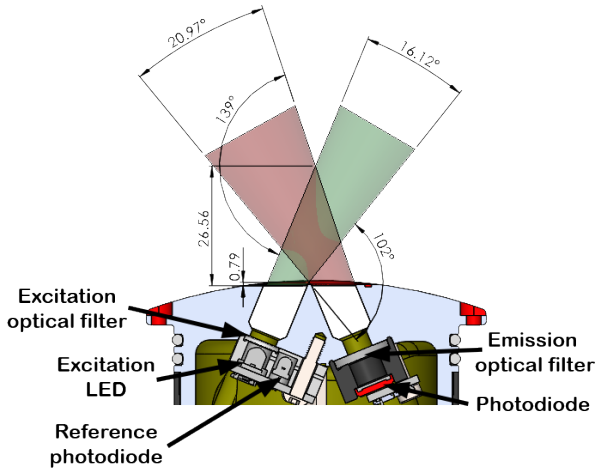

Fig. 1. Schematic of the RBR*tridente* showing the geometry of the sensing volumes. Light is emitted from the excitation side while light is detcted from the other side, referred to as the emission side for fluorometers and the detector side for backscatter sensors. The sensing volume located at the intersection of both excitation and emission cones forms a three-dimensional volume of 1.3 cm^3.

excitation LED's characteristics, as well as to compensate for the temperature dependence of the excitation LED. The light emitted back from the sample through fluorescence then passes through an emission optical filter that allows only the desired emitted wavelength to pass through, effectively blocking any residual excitation light, as well as ambient light. This filtered emission light is then detected by a photodiode, which converts the light signal into an electrical signal. This selective filtering is essential for accurate and reliable detection of the target fluorescence, allowing for precise quantification of substances such as chlorophyll, phycoerythrin, fDOM, and Rhodamine WT. The RBR*tridente* has the capabilities to target a series of fluorescent compounds through a set of Excitation/Emission pairs listed in Table I.

TABLE I
EXCITATION/EMISSION PAIRS USED BY THE RBR*tridente* DEPENDING ON THE TARGETTED VARIABLE.

Variable	Excitation Wavelength (nm)	Emission Wavelength (nm)
Chlorophyll-a	470	700
Chlorophyll-a	435	700
Phycoerythrin	525	600
Phycocyanin	590	654
fDOM	365	450
Rhodamine WT	550	600
Fluorescein	460	550

B. Backscatter

Backscatter sensors operate on the principle of light scattering to measure the concentration and characteristics of particulate matter in water. The construction of the sensor is similar to the one of the fluorometer shown in Fig. 1, except for the excitation optical filter that is not necessary for backscattering. The process begins with a light source, typically an LED, that emits a beam of light into the water. As this light travels through the water, it encounters particles that cause the light to scatter in various directions. The backscattered light, which is the portion of the scattered light that is redirected back towards the sensor, is detected by a photodiode located on the detector side. The detector side of the sensor includes an optical filter that ensures only the desired wavelengths of backscattered light reach the photodiode. These filters are crucial as they help eliminate interference from ambient light and other wavelengths that are not of interest. The intensity of the backscattered light is directly related to the concentration and size of the particles in the water. Several wavelengths are available on the RBR*tridente*: 470, 525, 650, and 700 nm. The LEDs characteristics for each of these wavelengths are presented in Table II. Using multiple wavelengths allows for a more comprehensive analysis of particulate matter, enabling the differentiation between various particle types and sizes.

TABLE II
CENTRAL WAVELENGTH AND FULL WIDTH AT HALF MAXIMUM (FWHM) OF THE EXCITATION LED AND PHOTODIODE FOR EACH BACKSCATTERING CHANNEL AVAILABLE ON THE RBR*tridente*.

Backscattering wavelength (nm)	Excitation central wavelength (nm)	Photodiode central wavelength (nm)
700	700 ± 19	695 ± 65
650	660 ± 17	650 ± 50
525	525 ± 35	525 ± 80
470	470 ± 20	470 ± 45

III. LABORATORY CALIBRATION PROCESS

The calibration protocol for both fluorescence and backscatter on the RBR*tridente* is a three-step process: The gain calibration, the temperature compensation, and the optical calibration. The first two steps are common to all calibrations for the RBR*tridente*, independently of the measured variables. The third one, the optical calibration, depends on the targetted variable (chlorophyll, backscatter, rhodamine WT, etc).

A. Gain calibration

The RBR*tridente* can operate in four different gains (1X, 10X, 100X, and 1000X) to capture the full range of expected values while preserving the sensitivity of the measurement at very low concentrations and avoid saturating the measurements at high concentrations. The appropriate gain is automatically determined at the beginning of each acquisition sequence. As a result, it is important to ensure that all gains are colinear, and transitions between gains show no steps in the data. The gain calibration includes the determination of both an offset and a scalar for each of the four gains.

The gain offset is determined in-air by covering the detectors with black opaque tape to collect "dark" data. 200 samples are collected in each of the four gains. The last 100 samples of each sampling phase are averaged to determine the gain offset for each of the four gains (Fig. 4).

The gain scalar is determined in-air using a plate that induces a static fluorescence or scattered signal. For chlorophyll

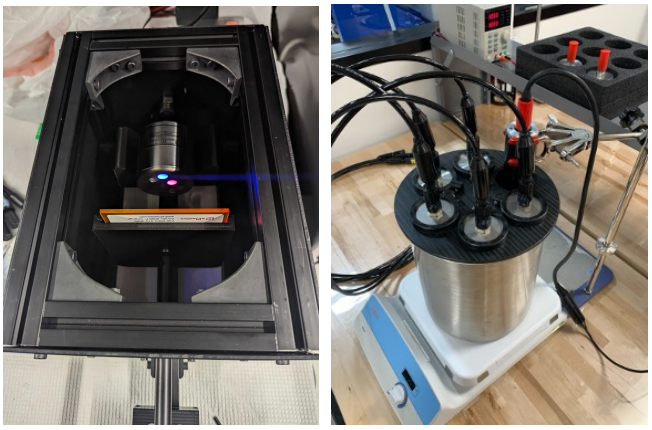

Fig. 2. [left] Gain calibration setup for the RBR*tridente*. The solid standard used for backscattering gain calibration is visible. [right] Optical calibration setup for backscattering. Six instruments are shown: five RBR*tridente* and the reference instrument: a LISST-TAU transmissometer (532 nm) (in the red clamp).

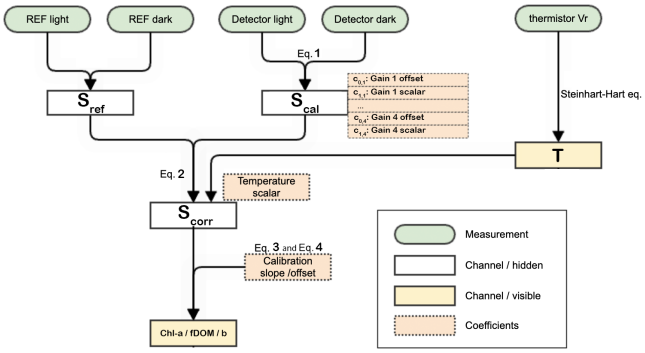

Fig. 3. Workflow from the measured signal from the reference photodiode (REF) and the detector photodiode (see Fig. 1). Variables names and key equations used throughout the workflow are detailed in the text. This diagram applies to both backscatter and fluorescence measured by the RBR*tridente*.

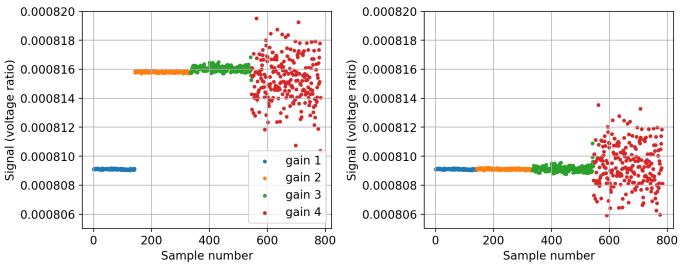

Fig. 4. Measured signal before (left) and after (right) gain calibration. The colinearity of the four different gains obtained after gain calibration is shown.

and backscattering sensor calibrations, the plate is an orange acrylic plate (9096 F), while a blue acrylic plate (9092 F) is used for fDOM. The plate is moved until the reading reaches 80% of gain 1000X. Readings from the plate are then taken at each gain (1000X,100X,10X,1X) following the same protocol as for the gain offset: the scalar is derived for each gain by taking the average reading over the last 100 samples in gain 1000X and dividing it by the average of the lat 1000 readings obtained at each gain (1000X, 100X, 10X, and 1X). The gain scalar must be between 0.98 and 1.02 ($\pm$ 2%) to fit within the tolerance of the resistors used for the different gains.

A total of eight coefficients are obtained. For each measurement obtained, the appropriate gain offset and scalar are applied to the reading as a first step (see Fig. 3). The reading from the photodiode is thus obtained following:

$$S_{cal} = c_{0,i} + c_{1,i} \times S_{raw} \tag{1}$$

where S_{raw} is the raw signal, $c_{0,i}$ and $c_{1,i}$ are the gain offset and scalar, respectively, at the gain i, and S_{cal} is the gain-adjusted signal.

B. Temperature compensation

The RBR*tridente* is equipped with an internal thermistor to monitor the internal temperature of the instrument. The temperature readings from that internal thermistor are used to compute a temperature-compensated signal from the RBR*tridente*, using:

$$S_{corr} = \frac{S_{cal}}{S_{ref}} \times (1 + X_1 \times (X_0 - T)) \tag{2}$$

where S_{corr} is the temperature-compensated signal, S_{ref} is the signal measured by the reference photodiode, X_1 and X_0 are calibration coefficients and T is the measured temperature in °C.

The calibration coefficients (X_0, X_1) are measured by splitting the working solution into three vessels: a cooled one, a heated one, and one at room temperature. The response of the instruments to the temperature step as it thermally equilibrates is analyzed to measure the linear temperature response.

The coefficient X_1 is derived from the slope of the relationship between temperature and S_{cal}, while X_0 is set to be the reference temperature set for calibration (15 °C). It is important to note that, while that step is part of the calibration process, the temperature dependence (X_1) for fluorescence is negligible compared to its uncertainties, and is therefore set to 0. This is thought to be because of the presence of the reference photodiode (see Fig. 1) used to reference the measured signal (Fig. 3). To the first order, the reference photodiode would have a similar temperature response as the detector photodiode.

C. Optical calibration

1) Fluorescence: A primary standard for each fluorescence parameter is established. This primary standard depends on the targeted variable (chlorophyll, fDOM, rhodamine, etc.). For example, for chlorophyll-a, the primary standard is formed from a chlorophyll-a pigment from Sigma-Aldrich (CAS Number: 479-61-8) suspended in 90% acetone. The primary standard is dissolved in a suitable medium and titrated to make a series of primary solutions across the full range of the expected concentrations for the parameter. In the case of

chlorophyll-a, a series of five solutions is formed at ∼50 μg/L increments. Using a spectrophotometer (Cary 3500 UV-Vis) as a primary reference instrument, the signal amplitude from the reference solutions is determined using the spectrophotometric method developed in [7]. A Secondary Reference Instrument (SRI) is calibrated in the chlorophyll-a pigment suspended in acetone, to be used to calibrate other RBR*tridente*. This 5-point calibration with the chlorophyll-a pigment has been repeated three times on three separate samples of the pigment, and produces calibration slopes that agree within 2%.

The same process is used to form a series of working solutions using a Fluorescein dye solution. The amplitudes of the working solutions are measured using the SRI to determine the equivalent chlorophyll concentration. Once the working solutions' chlorophyll equivalent concentrations have been derived, RBR*tridente*s are calibrated using these solutions. The SRI is also used to monitor the working solutions in the calibration process as the concentration will not be stable over time due to the degradation of the fluorescent pigment. Once a working solution is no longer within the 80% of the target calibration concentration, the working solution is discarded and a new one is produced.

Being able to use the RBR*tridente* directly in the primary standard suspended in acetone without altering its performance is a key benefit, and is not necessarily the case for other fluorometers and backscattering sensors commonly used in the ocean. It avoids relying on the spectrophotometer to characterize the working solution concentration. The use of the chlorophyll-a pigment and its quantization with the spectrophotometric method means that new primary standards can be acquired and quantified repeatedly at RBR, or in any other calibration facilities, which is important for the repeatability of the calibration procedure.

The optical calibration for fluorescence channels takes place in an 11.5 L (ø228.6 mm x 279.4 mm) cylindrical bath coated with black paint to minimize wall effects, similarly to what is shown in Fig. 2. A calibration sequence includes up to six instruments, with two SRIs and up to four RBR*tridente* to be calibrated. All instruments are aimed toward the center of the volume to avoid wall effects. Once the measurements are made in three of the working solutions, the linear relationship between the reported voltage and the equivalent concentration is used to calibrate the measured signal. For example, chlorophyll-a concentration would therefore be computed using the following equation:

$$chl\text{-}a = C_0 + C_1 \times S_{corr} \tag{3}$$

where $chl\text{-}a$ is the calibrated chlorophyll-a concentration, C_0 and C_1 are the offset and slope of the linear regression detailed above. The linear relationship is monitored by computing the coefficient of determination (R^2) that is found to be consistently >0.99. This calibration protocol will be identical independently of the targeted fluorescing compound, except for the primary standard used for the series of primary solutions: the primary standards are made from Quinine sulfate dihydrate (Fisher Scientific, CAS Number: 6119-70-6) for fDOM, 20% Rhodamine WT aqueous dye solution for rhodamine (Molekula Group, CAS Number: 37299-86-8), C-Phycocyanin (Sigma-Aldrich Ref. 52468) for phycocyanin, and R-Phycoerythrin (CAS Number: 11016-17-4) for phycoerythrin.

2) Backscatter: The objective of the calibration is to derive a scalar that can be used to convert the raw signal measured by the photodiode into the Volume Scattering Function (VSF), β, evaluated at a centroid angle, $\bar{\theta}$, in m^{-1} sr^{-1} [11]. The optical calibration of backscatter takes place in an identical cylindrical bath as for the fluorescence optical calibration. Each calibration sequence includes up to 6 instruments: one LISST-TAU transmissometer 532 nm used as a reference instrument, one calibrated RBR*tridente* to be used as an SRI, and up to four RBR*tridente* to be calibrated. The bath is filled with deionized (DI) water sourced from the laboratory's Milli-Q IX system. The DI water is guaranteed to have a conductance lower than 0.2 μS/cm and is left to acclimate overnight to room temperature to avoid degassing and minimize the formation of bubbles during calibration.

NIST-traceable 100 nm nanosphere beads (Thermofisher 3100A) are used to calibrate backscattering measurements. The beads are certified by the manufacturer to have a mean of 100 nm, with a dispersion (min to max) of 3 nm. Before being used for calibration, the beads are sonicated for 300 s to minimize bead clumps that could affect the measured signal during the calibration sequence. A magnetic stirrer is placed at the bottom of the bath to ensure beads are evenly distributed throughout the volume.

The calibration sequence is composed of a series of plateaus (8 to 10) that spans a range of transmission coefficients from 0 to 2.2 m^{-1}. Each plateau is reached by adding beads to the bath, followed by a stabilization period of 100 s. The next 25 s (100 samples) are averaged to obtain the reading for the plateau. At each plateau, the RBR*tridente* are powered sequentially to avoid cross-talk (electrical or optical) between the different sensors being calibrated.

After 3 plateaus, the slope of the linear relationship between the measured voltage from the RBR*tridente* and the transmission coefficient measured from the reference instrument is computed. This slope corresponds to the experimental backscatter phase function, $\tilde{\beta}_e(\bar{\theta}_i)$ [11]. The coefficient of determination (R^2) of the linear relationship is monitored for all subsequent plateaus to ensure linearity. Typically, R^2 is between 0.9999 and 1.0000. Several other quality control steps are taken during the calibration process: First, the measurements collected over each plateau must be stable (i.e., no drift). If a trend is detected, the calibration bath is inspected for air bubbles on the surface of the RBR*tridente*. Air bubbles tend to occur when the bath is not thermally equilibrated before calibration. Second, the noise level of the data collected over a calibration plateau is monitored. Higher noise could indicate a grounding issue or the presence of clumps in the beads used in the calibration bath.

The VSF $\beta(\bar{\theta}_i)$ is obtained using:

$$\beta(\bar{\theta}_i) = C_0 + C_1 \times S_{corr} \tag{4}$$

where S_{corr} is the temperature-compensated signal. C_1 is computed using

$$C_1 = \tilde{\beta}(\bar{\theta}_i)/\tilde{\beta}_e(\bar{\theta}_i) \tag{5}$$

where $\tilde{\beta}(\bar{\theta}_i)$ is the theoretical phase function, derived from the Mie theory using the beads properties, the LED spectral response, the water index of refraction, and the geometry of the RBR*tridente*. To ensure the repeatability of the calibration process, an RBR*tridente* was calibrated ten times over the span of 18 months. The spread in the measured linear slopes across all calibration sequences was 1.2%.

IV. Field-validation

A. Dataset and Methods

During a cruise onboard the *RV Investigator* in the Great Australian Bight in March 2024, an RBR*tridente* was repeatedly deployed on a shipboard CTD rosette to a depth of 6000 dbar. The ship's CTD rosette was equipped with an ECO-FLBB (SeaBird Scientific, SN6765) that measures chlorophyll-a and backscatter, as well as an ECO-FLCD (SeaBird Scientific, SN7138) measuring fDOM. The ECO FLBB was calibrated on October 4th, 2023, that is 5 months prior to the cruise, while the ECO FLCD was recalibrated on February 1st, 2024, only a few weeks before the cruise. An RBR*tridente* (RBR, SN211688) was mounted next to the ECO FLBB and ECO FLCD sensor for a direct comparison. ECO sensors sampled at 24 Hz, while the RBR*tridente* was set to sample at 8 Hz. No post-processing is applied to any of the datasets other than binning the profiles into 1 dbar bin in order to directly compare the data from the ECO sensors to the RBR*tridente*.

The backscattering coefficient b_b measured by the RBR*tridente* and the ECO FLBB are highly correlated (Figs. 5 and 6). The structure of the profile and the amplitude of the signal are in good agreement, as supported by the slope of the linear regression performed on the binned backscattering data (0.940; Fig. 6). The larger spikes seen in backscatter are expected and hypothesized to contain information on larger particles traveling through the measurement volume [4]. These spikes do not co-occur in the ECO FLBB and RBR*tridente* datasets, as the two sensors were horizontally placed about 60 cm away from each other, and are expected to sample different water parcels. This explains the larger deviations from the 1:1 line shown in Fig. 6 and the need to apply the linear model to the despiked data. The noise levels of the two sensors at depths greater than 3000 dbar are quite similar, with a standard deviation of 1.15×10^{-5} and 0.81×10^{-5} $\mathrm{m^{-1}sr^{-1}}$ for the RBR*tridente* and the ECO FLBB, respectively.

The chlorophyll-a concentrations measured by the two sensors present a strong relationship (Figs. 5 and 6). The linear fit between the RBR*tridente* and the ECO FLBB yields an offset of 0.014 μg/L, which is of the same order of magnitude as the detection limit of either instrument (0.01 μg/L). The

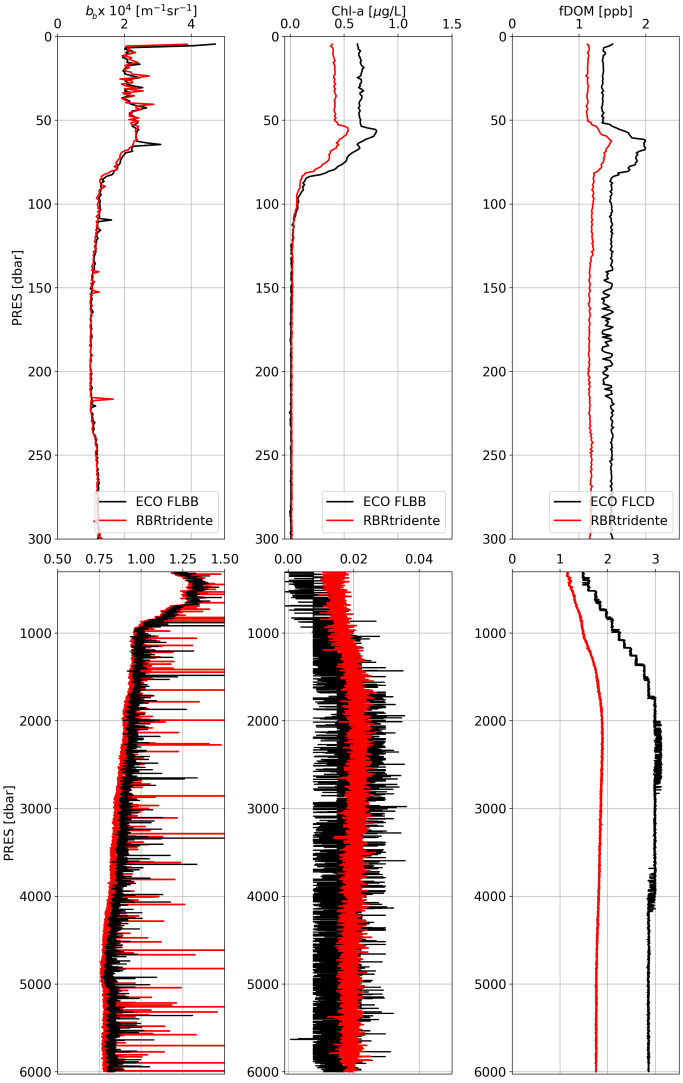

Fig. 5. Example of a profile collected onboard the *RV Investigator* (IN2024_T01, profile 4) for [left] backscattering coefficient b_b, [center] chlorophyll-a, and [right] fDOM. The red line shows the data from the RBR*tridente*, while the black line shows the data from the ECO FLBB and ECO FLCD colocated on the ship's CTD rosette. The top panels focus on the top 300 dbar, while the bottom panels show the rest of the profile, down to 6000 dbar.

small offset suggests that the dark calibration is performing consistently between the two instruments. The slope of 1.56, on the other hand, highlights a discrepancy between the two instruments. This slope, however, falls within the range of observed biases for the ECO sensors [1]: [9] documents regional biases in the chlorophyll-a measured by ECO sensors ranging from 0.65 $\pm$ 0.03 in the Black Sea to 4.30 $\pm$ 1.36 in the Southern Ocean. The noise level observed at depth for chlorophyll-a is almost three times smaller on the RBR*tridente* than for ECO FLBB. Below 3000 dbar, the standard deviation in chlorophyll-a measurements are 0.0018 and 0.0052 μg/L for the RBR*tridente* and the ECO FLBB, respectively. The larger noise level for the ECO FLBB could be partially due to the scalar difference observed with the RBR*tridente* of 1.6. A low

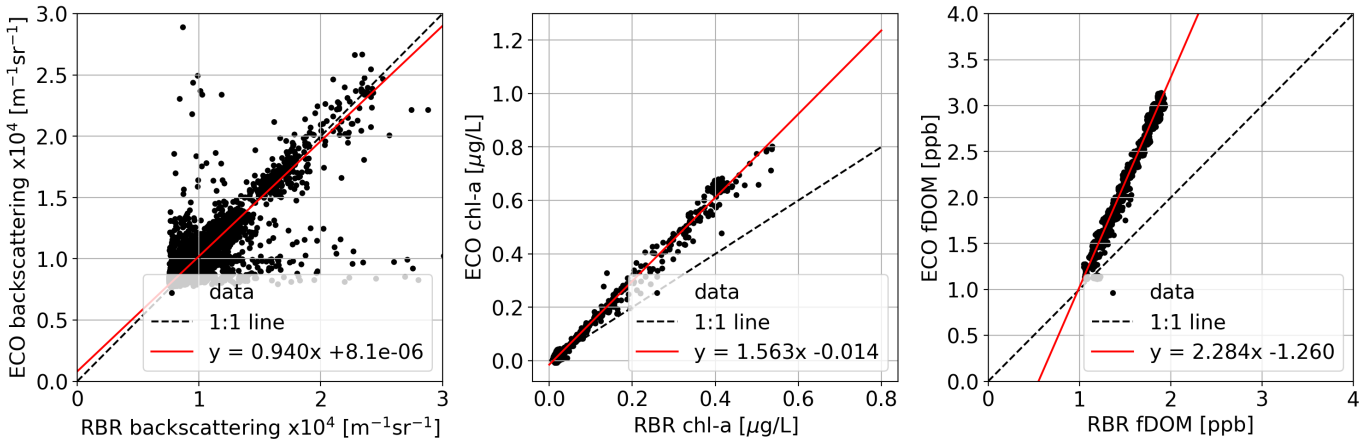

Fig. 6. Comparison of backscattering coefficient, chlorophyll-a, and fDOM measurements collected from the ECO FLBB or ECO FLCD versus the RBR*tridente* during the IN2024_T01 cruise onboard the *RV Investigator*. The 1:1 line is shown as a dashed line, while a linear regression between the two instruments is shown in red.

concentration, however, the lower resolution of the ECO FLBB also becomes apparent, with step changes in the chlorophyll-a values, which might also contribute to the larger standard deviation observed at depth.

Just like for chlorophyll-a, fDOM concentrations from the ECO FLCD and RBR*tridente* are strongly correlated (Figs. 5 and 6). However, both the offset and slope greatly differ between the two instruments, with the ECO FLCD consistently measuring higher fDOM concentrations. The linear fit between the two instruments yields an offset of -1.260 ppb and a slope of 2.284. The resolution of the fDOM measured by the ECO FLCD appears clearly in the data as step changes in the fDOM values. The ECO FLCD also shows higher noise (0.06 ppb) than the RBR*tridente* (0.03 ppb) at depths greater than 3000 dbar, although that might be due to the 2.284 slope factor showed in fig. 6.

V. Discussions and Conclusions

This study details the calibration procedure for the RBR*tridente*, a combined fluorescence-backscattering sensor developed by RBR. The three main steps of the calibration procedure (gain calibration, temperature compensation, and optical calibration) are individually described, providing all details to be replicable. The gain calibration assures a smooth transition across all four gains available on the RBR*tridente*, which is verified in the field, where no transition is observed despite sampling through large gradients. The temperature calibration is included in the calibration process, thanks to a thermistor included inside the RBR*tridente*. However, the temperature dependence measured in the laboratory is smaller than its uncertainties. As a result, the temperature compensation is set to zero, as it could otherwise introduce more errors into the final estimates. The reason for this weak temperature dependence is the presence of a reference photodiode that is expected to have a similar temperature response as the detector photodiode. The optical calibration differs for fluorometers and backscatter sensors, but both established protocols show encouraging repeatability over time, across primary standards, and over multiple calibration sequences. This is a crucial component to ensure consistency in the data collected with the RBR*tridente* across units and over time, particularly in the context of the recent discovery of large inconsistencies in fDOM measurements [10].

The field-validation of the RBR*tridente* yields encouraging results regarding the quality of the calibration procedure, despite lacking a robust reference. Field efforts should be directed toward collecting a complete and robust dataset to better characterize the quality of the calibration procedure, across several manufacturers, but also across instruments of a single manufacturer. Future improvments will be focusing on reducing the uncertainties in characterizing the temperature dependence of the sensors in order to gain confidence in the temperature compensation calibration step. A community effort towards unifying the calibration procedures across manufacturers to ensure the homogeneity of the global datasets is also a critical path of improvement [5]. The degree to which fluorometers calibrated with a live culture versus a chlorophyll-a can be compared remains poorly-constrained.

Documenting calibration procedures is a key aspect of ensuring transparency and interoperability across sensor manufacturers. This transparency is particularly important for large-scale, long-term monitoring programs like the BGC-Argo program, where the consistency and comparability of data over time and across different sensors are critical. By providing detailed documentation, we promote the reproducibility of calibration methods, allowing other researchers and manufacturers to adopt similar standards or compare methodologies. This contributes to the overall quality and reliability of the data collected, to the benefit of the oceanographic community.

Acknowledgment

We would like to acknowledge the BGC-Argo Technical Task Team for their invaluable assistance in narrowing down

the critical details of the RBR*tridente*'s calibration procedure. We also thank Alex Duran for providing additional key information that significantly enhanced the depth and comprehensiveness of this work.

REFERENCES

[1] Schmechtig Catherine and Claustre Herve and Poteau Antoine and D'Ortenzio Fabrizio and Schallenberg Christina and Trull Thomas and Xing Xiaogang. BGC-Argo quality control manual for the Chlorophyll-A concentration. Technical report, Ifremer, 2023.

[2] Sonia Batten and Sanae Chiba and David Checkley. Essential Ocean Variables (EOV) for Biology and Ecosystems: Zooplankton biomass and diversity. Technical report, The Global Ocean Observing System (GOOS), 2019.

[3] Henry C. Bittig, Tanya L. Maurer, Joshua N. Plant, Catherine Schmechtig, Annie P. S. Wong, Hervé Claustre, Thomas W. Trull, T. V. S. Udaya Bhaskar, Emmanuel Boss, Giorgio Dall'Olmo, Emanuele Organelli, Antoine Poteau, Kenneth S. Johnson, Craig Hanstein, Edouard Leymarie, Serge Le Reste, Stephen C. Riser, A. Rick Rupan, Vincent Taillandier, Virginie Thierry, and Xiaogang Xing. A BGC-Argo Guide: Planning, Deployment, Data Handling and Usage. *Frontiers in Marine Science*, 6, 2019.

[4] Nathan Briggs, Mary Jane Perry, Ivona Cetinić, Craig Lee, Eric D'Asaro, Amanda M. Gray, and Eric Rehm. High-resolution observations of aggregate flux during a sub-polar north atlantic spring bloom. *Deep Sea Research Part I: Oceanographic Research Papers*, 58:1031–1039, 10 2011.

[5] Zachary K. Erickson, Ivona Cetinić, Xiaodong Zhang, Emmanuel Boss, P. Jeremy Werdell, Scott Freeman, Lianbo Hu, Craig Lee, Melissa Omand, and Mary Jane Perry. Alignment of optical backscatter measurements from the exports northeast pacific field deployment. *Elementa: Science of the Anthropocene*, 10, 3 2022.

[6] Frank Muller-Karger and Raphael Kudela. Essential Ocean Variables (EOV) for Biology and Ecosystems: Phytoplankton biomass and diversity. Technical report, The Global Ocean Observing System (GOOS), 2016.

[7] SW Jeffrey and GF Humphrey. New spectrophotometric equations for determining chlorophylls a, b, c1 and c2 in higher plants, algae and natural phytoplankton. *Biochemie und physiologie der pflanzen*, 167(2):191–194, 1975.

[8] Line Bourdages and Artur Palacz. Essential Ocean Variable (EOV): Particulate Matter. Technical report, The Global Ocean Observing System (GOOS), 2017.

[9] Collin Roesler, Julia Uitz, Hervé Claustre, Emmanuel Boss, Xiaogang Xing, Emanuele Organelli, Nathan Briggs, Annick Bricaud, Catherine Schmechtig, Antoine Poteau, Fabrizio D'Ortenzio, Josephine Ras, Susan Drapeau, Nils Haëntjens, and Marie Barbieux. Recommendations for obtaining unbiased chlorophyll estimates from in situ chlorophyll fluorometers: A global analysis of wet labs eco sensors. *Limnology and Oceanography: Methods*, 15:572–585, 6 2017.

[10] Sea-Bird Electronic, Inc. Reported bias in measurements from sea-bird scientific cdom fluorometers. Technical report, Sea-Bird Electronic, Inc., 2023.

[11] James M. Sullivan, Michael S. Twardowski, J. Ronald, V. Zaneveld, and Casey C. Moore. *Measuring optical backscattering in water*, pages 189–224. Springer Berlin Heidelberg, Berlin, Heidelberg, 2013.